Active DNA demethylation in plant companion cells reinforces transposon methylation in gametes

Ibarra, Christian A ; Feng, Xiaoqi ; Schoft, Vera K ; Hsieh, Tzung-Fu ; Uzawa, Rie ; Rodrigues, Jessica A ; Zemach, Assaf ; Chumak, Nina ; Machlicova, Adriana ; Nishimura, Toshiro ; Rojas, Denisse ; Fischer, Robert L ; Tamaru, Hisashi ; Zilberman, Daniel

Abstract: The Arabidopsis thaliana central cell, the companion cell of the egg, undergoes DNA demethylation before fertilization, but the targeting preferences, mechanism, and biological significance of this process remain unclear. Here, we show that active DNA demethylation mediated by the DEMETER DNA glycosylase accounts for all of the demethylation in the central cell and preferentially targets small, AT-rich, and nucleosome-depleted euchromatic transposable elements. The vegetative cell, the companion cell of sperm, also undergoes DEMETER-dependent demethylation of similar sequences, and lack of DEMETER in vegetative cells causes reduced small RNA-directed DNA methylation of transposons in sperm. Our results demonstrate that demethylation in companion cells reinforces transposon methylation in plant gametes and likely contributes to stable silencing of transposable elements across generations.

DOI: https://doi.org/10.1126/science.1224839

DEMETER-mediated active DNA demethylation in *Arabidopsis thaliana* companion cells reinforces transposon methylation in gametes

Christian A. Ibarra[1*], Vera K. Schoft[2*], Tzung-Fu Hsieh[1*], Xiaoqi Feng[1*], Rie Uzawa[1*], Assaf Zemach[1], Nina Chumak[2], Adriana Machlicova[2], Toshiro Nishimura[1], Jessica A. Rodrigues[1], Denisse Rojas[1], Robert L. Fischer[1†], Hisashi Tamaru[2†], Daniel Zilberman[1†]

[1]Department of Plant and Microbial Biology, University of California, Berkeley, CA, USA.

[2]Gregor Mendel Institute, Austrian Academy of Sciences, Vienna, Austria.

[*]These authors contributed equally.

[†]To whom correspondence should be addressed. E-mail: rfischer@berkeley.edu, hisashi.tamaru@gmi.oeaw.ac.at, danielz@berkeley.edu.

Abstract

The *Arabidopsis thaliana* central cell, the companion cell of the egg, undergoes DNA demethylation prior to fertilization. Active and passive mechanisms have been proposed to contribute to this process, and the targeting preferences, if any, and biological significance, of central cell demethylation remain unclear. Here, we show that active DNA demethylation mediated by the DEMETER DNA glycosylase accounts for all of the demethylation in the central cell, and preferentially targets small, AT-rich and nucleosome-depleted transposable elements. We also show that the vegetative cell, the companion cell of sperm, undergoes DME-dependent demethylation of similar sequences. We find that small RNA molecules can travel from the central cell to the egg, and that lack of DEMETER in vegetative cells causes reduced small RNA-directed DNA methylation of transposons in sperm. Our results demonstrate that demethylation in companion cells reinforces transposon methylation in plant gametes, thereby assuring stable silencing of transposable elements across generations.

Summary

Active DNA demethylation in the companion cells of plant gametes mediates stable trans-generational silencing of transposable elements.

Cytosine methylation regulates gene expression and represses transposable elements (TEs) in plants and vertebrates (*1*). DNA methylation in plants is catalyzed by three families of DNA methyltransferases that can be roughly grouped by the preferred sequence context: CG, CHG, and CHH (H = A, C or T). The small RNA (sRNA) pathway targets *de novo* methylation in all sequence contexts, and is required for the maintenance of CHH methylation. Plant DNA methylation patterns tend to be similar across tissues, with the exception of the developing seed (*2-4*).

Flowering plant sexual reproduction involves two fertilization events (*5*). The pollen vegetative cell forms a tube that carries two sperm cells to the ovule, where one fuses with the diploid central cell to form the triploid placenta-like endosperm, and the other fertilizes the haploid egg to produce the embryo. Endosperm DNA of *Arabidopsis thaliana* is modestly but globally less methylated than embryo DNA in all contexts (*3*). The *DEMETER* (*DME*) DNA glycosylase that excises 5-methylcytosine is highly expressed in the central cell prior to fertilization and is at least partially required for the demethylation observed in endosperm (*2, 3*), which has been inferred to occur on the maternal chromosomes inherited from the central cell. Passive mechanisms, such as downregulation of the *MET1* DNA methyltransferase, have also been proposed to contribute to demethylation of the maternal endosperm genome (*6*). The global differences between embryo and endosperm are consistent with passive demethylation, and suggest that the process may have little sequence specificity (*3, 7*). However, DNA methylation has not been compared between the maternal and paternal endosperm genomes except for a few loci, and therefore it is difficult to make general inferences about the mechanism and specificity of central cell demethylation. Why the central cell should undergo extensive DNA demethylation is also unclear.

To understand the extent, mechanism and biological significance of active demethylation in the central cell, we used reciprocal crosses between the Col and L*er* accessions of *A. thaliana* that differ by over 400,000 single nucleotide polymorphisms (SNPs) (*7*) to identify DNA methylation that resides on either the maternal or paternal endosperm genome (*8*) by shotgun bisulfite sequencing (table S1). The wild-type maternal genome is substantially less methylated than the paternal genome in the CG context (Fig. 1A and S1-2), with slight global hypomethylation accompanied by strong local demethylation in genes and transposons (Fig. 1B and S3-4). The local demethylation is nearly fully reversed in *dme* mutant endosperm (Fig. 1A-B, S2 and S4-5), indicating that DME is either the only or by far the major enzyme required for excision of 5-methylcytosine in the central cell, and demonstrating that active DNA demethylation of specific sequences accounts for the methylation differences between the maternal and paternal endosperm genomes. Global CG methylation of both maternal and paternal genomes is slightly elevated by lack of DME compared to wild type (Fig. 1A and S5), consistent with overexpression of genes that maintain CG methylation in *dme* endosperm (*7*).

Global CHG methylation of the wild-type endosperm maternal genome is similar to that of the paternal genome (Fig. 1C-D), but loci that are maternally demethylated in the CG context show strong maternal CHG demethylation (Fig. 1D), consistent with the reported *in vitro* activity of DME on methylation in all sequence contexts (*9*). A similar but weaker correspondence exists for CHH methylation (Fig. 1E-F), presumably because sRNA-directed DNA methylation patterns are partially restored after fertilization. As we showed previously, *dme* endosperm has greatly reduced CHG methylation and almost no CHH methylation (*3*), and our present data show that this applies similarly to both parental genomes (Fig. 1C, E and S2). As expected, we

did not observe major methylation differences between parental genomes in embryo (Fig. 1A, C, E, S1-2, S4 and S6).

Several TEs were reported to be less methylated in the pollen vegetative cell of *A. thaliana* compared to sperm (*10*), and we recently showed that DME is required for demethylation of two genes in the vegetative cell that are demethylated by DME in the central cell (*11*). These data suggest that DME-mediated DNA demethylation may proceed similarly in the central and vegetative cells. To examine this issue, we compared DNA methylation patterns in *A. thaliana* sperm and vegetative cell nuclei that were purified by fluorescence activated cell sorting (*11, 12*). Most CG sites are heavily and similarly methylated in both cell types, but a subset is specifically demethylated in the vegetative cell (Fig. 2A-B, S4 and S7). The demethylated vegetative cell CG sites strongly overlap those demethylated in the maternal endosperm genome, and by extension in the central cell (Fig. 2B and S4). We could not examine DNA methylation in pollen from homozygous *dme* plants because strong *dme* loss-of-function alleles are lethal when maternally inherited (*13*). Instead, we examined methylation in pollen from heterozygous *dme* plants, in which half of the pollen grains lack DME (*11*). CG sites that are demethylated in wild-type vegetative cells showed much greater methylation in vegetative cell nuclei isolated from heterozygous *dme* pollen (Fig. 2A-B, S4 and S7), indicating that DME is required for demethylation in the vegetative cell. CHG methylation is generally higher in the vegetative cell than in the sperm cell (Fig. 2C-D), but loci demethylated at CG sites in the vegetative cell are also demethylated at CHG sites (Fig. 2D), as they are in endosperm (Fig. 1D). CHH methylation shows more dramatic differences, with very high levels in the vegetative cell and low levels in sperm (Fig. 2E), though vegetative cell CG-demethylated loci tend to show lower levels of CHH methylation in vegetative cells than in sperm (Fig. 2F). Overall, our data

strongly support the hypothesis that DNA demethylation in the male and female companion cells proceeds by an active, DME-dependent mechanism.

Loci demethylated in *A. thaliana* central and vegetative cells tend to be within AT-rich TEs smaller than 500 bp that are depleted of nucleosomes dimethylated at lysine 9 of histone H3 (Fig. 3A-E and S8), suggesting that chromatin structure plays an important role in regulating active DNA demethylation. TEs longer than 3 kb are rarely demethylated (fig. S3), except at the edges (Fig. 3F), consistent with our published observations in rice (*4*). The preference for smaller TE demethylation is stronger in endosperm than in pollen (Fig. 3A-B, G ($p<0.001$, Kolmogorov-Smirnov test) and S3), potentially reflecting chromatin differences between central and vegetative cells. Small *A. thaliana* TEs, like their rice counterparts (*4*), tend to occur near genes (Fig. 3H), explaining the observation that DME and related glycosylases preferentially demethylate gene-adjacent sequences (Fig. 3H) (*2, 14, 15*).

DME-mediated DNA demethylation in the central cell is required to establish monoallelic (imprinted) expression of a number of genes in the endosperm (*5, 7*), but the abundance of DME targets in gene-poor heterochromatin (fig. S9) and the overlap among DME targets in the central and vegetative cells, despite their different functions and developmental fates, suggest that establishment of genomic imprinting is not the basal function of DME. DNA demethylation of TEs in the vegetative cell was proposed to generate sRNAs that would reinforce silencing of complementary TEs in sperm (*10*). We tested whether sRNAs can travel from the central cell to the egg by specifically expressing a microRNA in the central cell that targets cleavage of GFP RNA expressed from a transgene in the egg, analogous to an experiment performed earlier in pollen (*10*). The central cell-specific mircoRNA substantially reduced

expression of GFP in the egg (Fig. 4A-B and table S2), suggesting that central cell sRNAs can travel into and function in the egg.

If silencing induced by companion cell sRNAs occurs at the transcriptional level, lack of DME in the companion cell would be expected to reduce sRNA-directed CHH methylation of DME target sequences in gametes. Indeed, CG sites demethylated by DME in vegetative cells show CHH hypomethylation in heterozygous *dme* sperm (Fig. 4C). Conversely, loci that exhibit decreased CHH methylation in heterozygous *dme* sperm show increased CG methylation in heterozygous *dme* vegetative cells (Fig. 4D-E). Thus, DME activity in the vegetative cell is required for full methylation of a subset of sperm TEs.

We have shown that DME mediates extensive DNA demethylation of small TEs in the companion cells of male and female gametes (Fig 1-3). Lack of demethylation reduces DNA methylation of cognate gamete TEs (Fig. 4C-E), indicating that demethylation in companion cells generates a mobile signal that acts in gametes. sRNA, which can move between cells and is the best candidate for such a signal (*16*), is able to travel from the vegetative cell to the sperm (*10*) and from the central cell to the egg (Fig. 4A-B). Thus, active demethylation in companion cells effectively generates a vaccine (sRNA) that immunizes the gametes against TE activation, maintaining stable TE repression across generations.

References

1. J. A. Law, S. E. Jacobsen, *Nature Reviews Genetics* **11**, 204 (2010).
2. M. Gehring, K. L. Bubb, S. Henikoff, *Science* **324**, 1447 (2009).
3. T.-F. Hsieh *et al.*, *Science* **324**, 1451 (2009).
4. A. Zemach *et al.*, *Proc Natl Acad Sci U S A* **107**, 18729 (2010).
5. J. H. Huh, M. J. Bauer, T.-F. Hsieh, R. L. Fischer, *Cell* **132**, 735 (2008).
6. P. E. Jullien *et al.*, *PLoS Biol* **6**, e194 (2008).
7. T. F. Hsieh *et al.*, *Proc Natl Acad Sci U S A* **108**, 1755 (2011).
8. Materials and methods are available as supporting material on Science Online.
9. M. Gehring *et al.*, *Cell* **124**, 495 (2006).
10. R. K. Slotkin *et al.*, *Cell* **136**, 461 (2009).
11. V. K. Schoft *et al.*, *Proc Natl Acad Sci U S A* **108**, 8042 (2011).
12. V. K. Schoft *et al.*, *EMBO Rep* **10**, 1015 (2009).
13. Y. Choi *et al.*, *Cell* **110**, 33 (2002).
14. R. Lister *et al.*, *Cell* **133**, 395 (2008).
15. J. Penterman *et al.*, *Proc Natl Acad Sci U S A* **104**, 6752 (2007).
16. S. A. Simon, B. C. Meyers, *Curr Opin Plant Biol* **14**, 148 (2011).
17. We thank the BioOptics team at the Vienna Biocenter Campus for isolation of vegetative cell nuclei and sperm cells, Keith Slotkin for the *LAT52p-amiRNA=GFP* plasmid, and Gary Drews for the *DD45p-GFP* transgenic line. This work was partially funded by an NIH grant (GM69415) to Robert Fischer, NSF grants (MCB-0918821 and IOS-1025890) to Robert Fischer and Daniel Zilberman, a Young Investigator Grant from the Arnold and Mabel Beckman Foundation to Daniel Zilberman, an Austrian Science Fund (FWF) grant P21389-B03 to Hisashi Tamaru, a Ruth L. Kirschstein NIH Predoctoral Fellowship (GM093633) to Christian Ibarra, a Fulbright Scholarship to Jessica Rodrigues, and a fellowship from the Jane Coffin Childs Memorial Fund to Assaf Zemach. Sequencing data are deposited in GEO with accession number GSExxxxx.

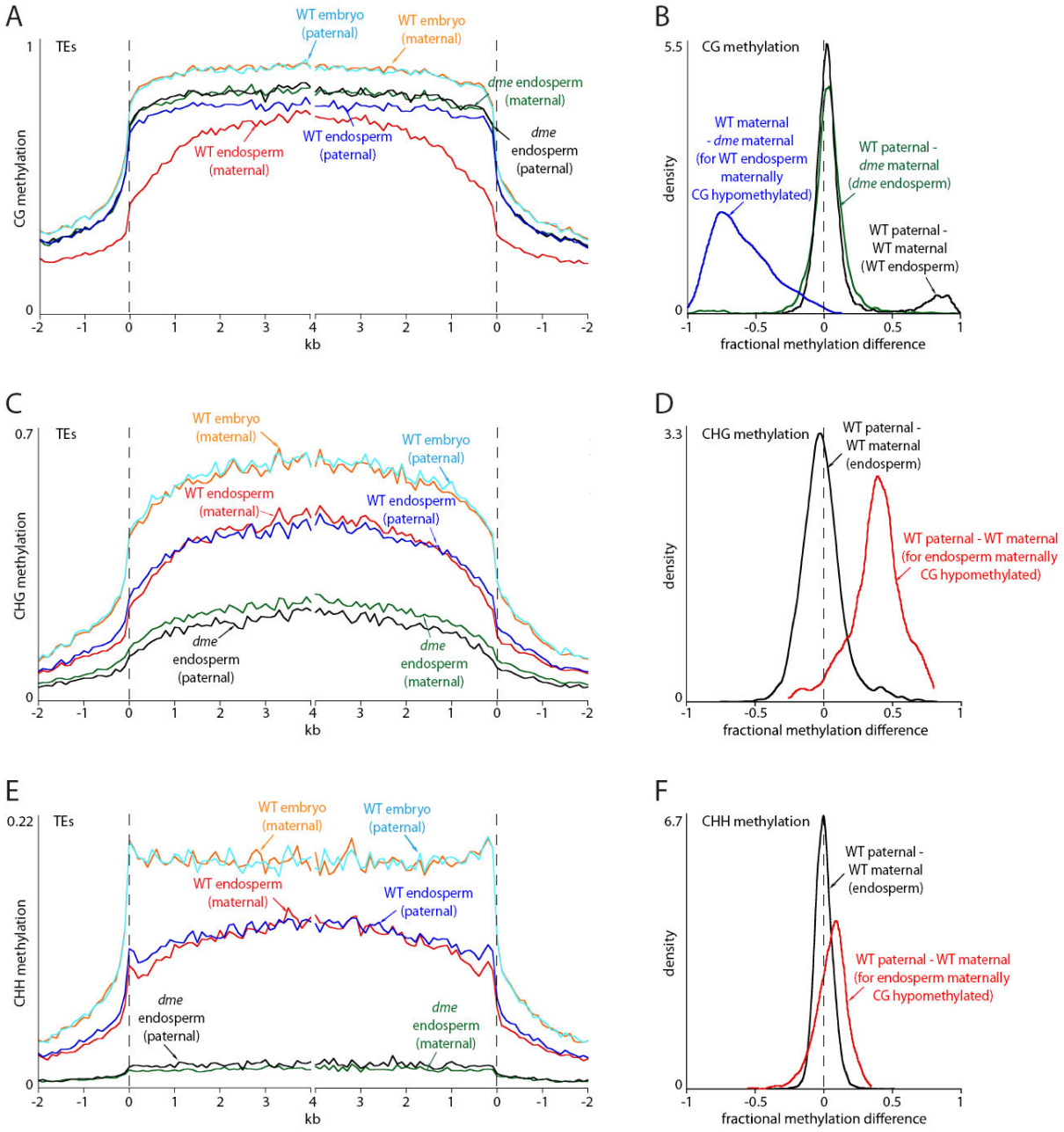

Fig. 1. Local DME-dependent demethylation of maternal endosperm chromosomes. (**A, C, E**) Transposons were aligned at the 5' and 3' ends (dashed lines) and average methylation levels for each 100-bp interval are plotted. (**B, D, F**) Kernel density plots of endosperm methylation differences. A shift of the peak with respect to zero represents a global difference; shoulders represent local differences.

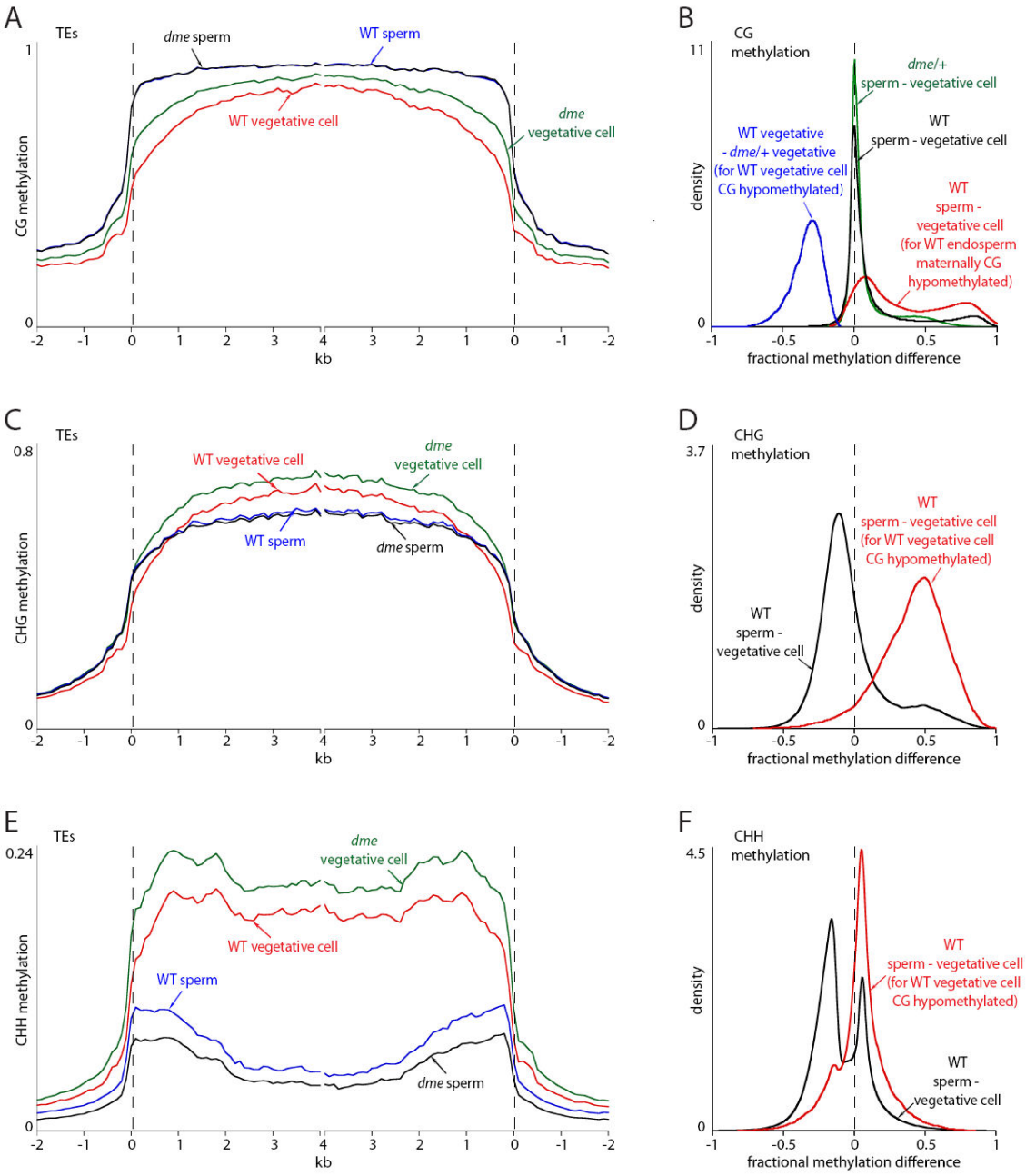

Fig. 2. Local DME-dependent demethylation in the pollen vegetative cell. (**A, C, E**) Average methylation in transposons was plotted as in Fig. 1. (**B, D, F**) Kernel density plots of pollen methylation differences. A shift of the peak with respect to zero represents a global difference; shoulders represent local differences.

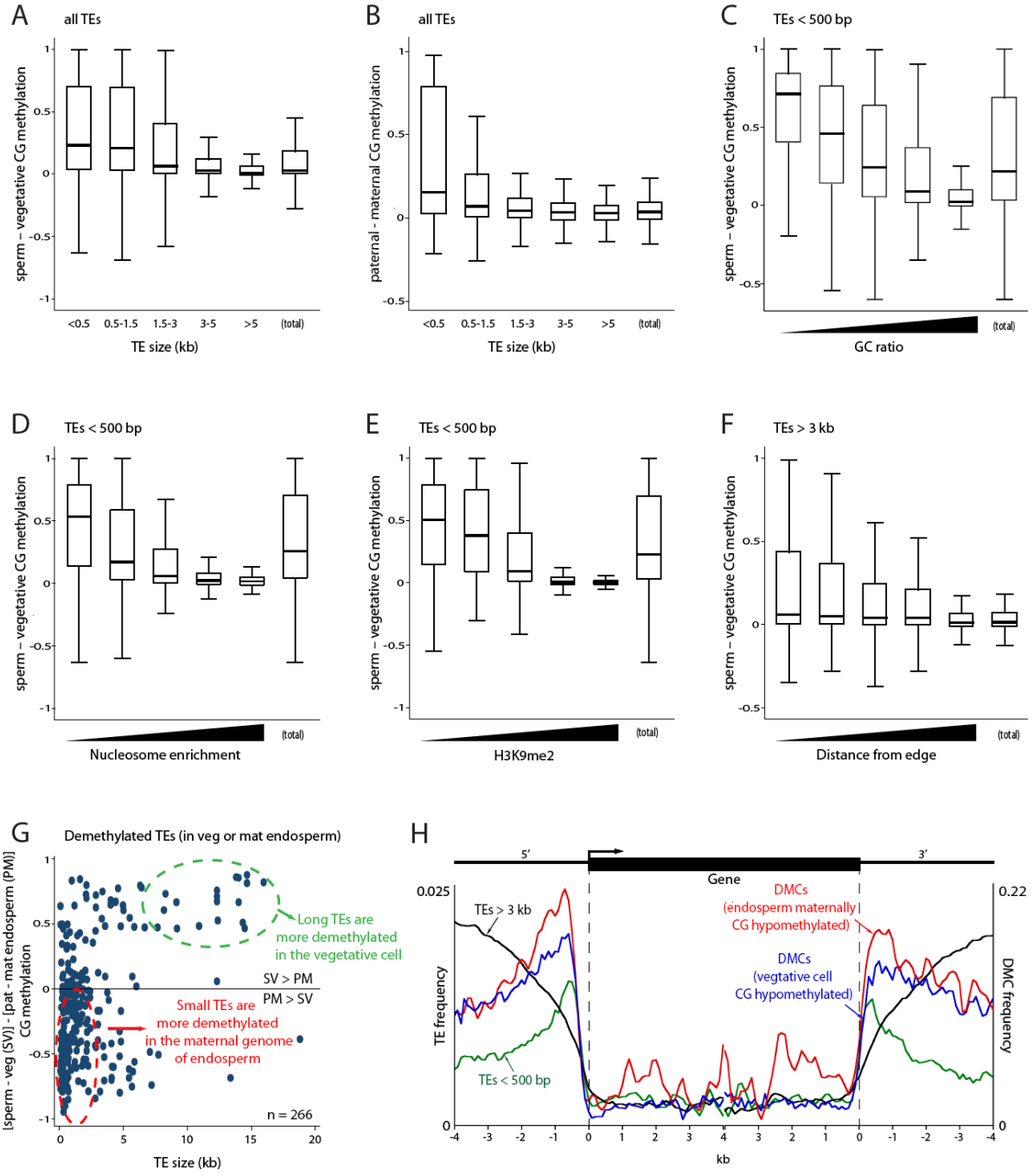

Fig. 3. DME demethylates small, AT-rich and nucleosome-poor TEs. (**A-F**) Box plots showing the extent of demethylation in transposons. Each box encloses the middle 50% of the distribution, with the horizontal line marking the median, and vertical lines marking the minimum and maximum values that fall within 1.5 times the height of the box. (**G**) Scatter plot of demethylation differences between pollen and endosperm. (**H**) Distribution of transposable elements and significantly differentially methylated cytosines (DMCs; CG context; p-value < 0.0001, Fisher's exact test) with respect to genes.

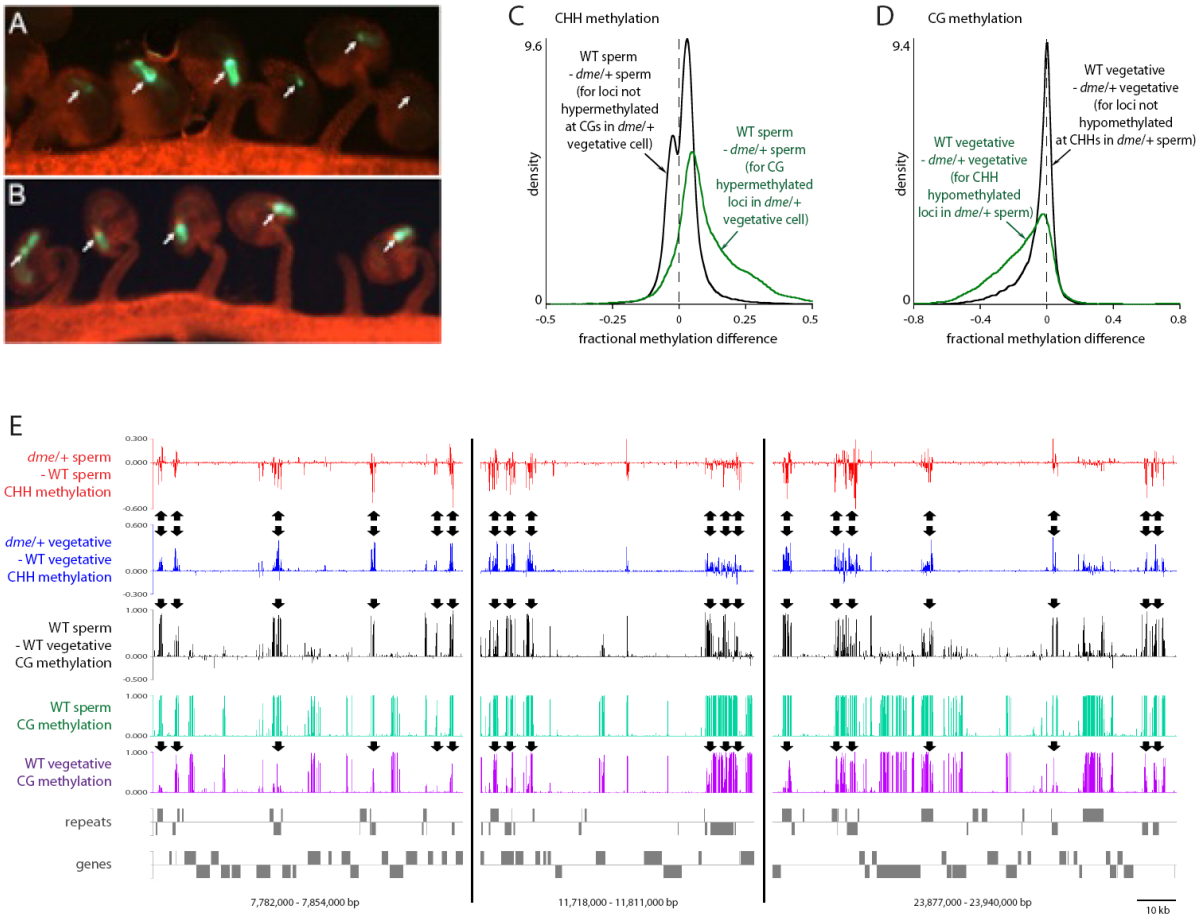

Fig. 4. Demethylation of small TEs in vegetative cells reinforces methylation in sperm. (**A-B**) Egg cell GFP expression in a plant line (table S2, line 2) hemizygous for a transgene expressing and anti-GFP microRNA in the central cell (**A**) and a control line (table S2, line 7) lacking the microRNA (**B**). Arrows point to egg cells. (**C**) Kernel density plots of the CHH methylation differences between sperm cells from wild-type and heterozygous *dme* plants. (**D**) Kernel density plots of the CG methylation differences between vegetative cells from wild-type and heterozygous *dme* plants. (**E**) Snapshots of CG and CHH methylation in pollen on chromosome 1. Arrows point out loci with decreased CHH methylation in sperm and increased CG methylation in vegetative cells from heterozygous *dme* pollen.

Supporting online material

Materials and methods

Isolation of *A. thaliana* endosperm. Stage 12-13 flower buds were emasculated and pollinated 48 hours later. Reciprocal crosses were performed using wild-type Col-0 and L*er* ecotypes. In addition, *dme-2* (Col-*gl*) (*S1*) heterozygous flowers were pollinated with wild-type (L*er*) pollen. For wild-type crosses, seven to eight days after pollination, F1 seeds (torpedo-stage to early-bent-cotyledon stage) were immersed in 0.3 M sorbitol and 5 mM Mes (pH 5.7) on a slide under a dissecting microscope. Embryo and endosperm were dissected using a fine needle and forceps. The seed coat was discarded. Wild-type embryos were twice centrifuged and the pellet resuspended in 0.3 M sorbitol and 5 mM Mes (pH 5.7) to remove contaminating endosperm. For crosses with the *dme-2* mutation, F1 aborting seeds were identified and mutant endosperm was isolated. Approximately 500 wild-type endosperm, 1000 *dme-2* endosperm, and 300 wild-type embryos were collected.

Isolation of vegetative nuclei and sperm cells. Pollen was isolated from wild-type (Col-0) and *dme-2* heterozygous plants (Col-*gl* ecotype) as described previously (*S2, S3*). Vegetative cell nuclei and sperm cells were extracted from mature pollen and fractionated by fluorescence activated cell sorting as described previously (*S2, S3*).

Bisulfite sequencing library construction. As described previously, genomic DNA was isolated from vegetative nuclei and sperm cells (*S2*), endosperm, and embryo (*S4*). Paired-end bisulfite sequencing libraries for Illumina sequencing were constructed as described previously (*S4*) with minor modifications. In brief, about 150 ng of genomic DNA was fragmented by sonication, end repaired and ligated to custom-synthesized methylated adapters (Eurofins MWG Operon) according to the manufacturer's (Illumina) instructions for gDNA library construction. Adaptor-ligated libraries were subjected to two successive treatments of sodium bisulfite conversion using the EpiTect Bisulfite kit (Qiagen) as outlined in the manufacturer's instructions. One quarter of the bisulfite-converted libraries was PCR amplified using the following conditions: 2.5 U of ExTaq DNA polymerase (Takara Bio), 5 µl of 10X Extaq reaction buffer, 25 µM dNTPs, 1 µl Primer 1.1, 1 µl Primer 2.1 (50 µl final). PCR reactions were carried out as follows: 95 □C 3 min, then 12-14 cycles of 95 □C 30 sec, 65 □C 30 sec and 72 □C 60 sec. The enriched libraries were purified twice with solid phase reversible immobilization (SPRI) method using AM-Pure beads (Beckman Coulter) prior to quantification with a Bioanalyzer (Agilent). Sequencing on the Illumina platform was performed at the Vincent J. Coates Genomic Sequencing Laboratory at UC Berkeley and the Genome Center at UC Davis.

Allele-specific determination of DNA methylation. Reads were sorted to the Col and L*er* genomes as described (*S5*). DNA methylation of cytosines within sorted reads was calculated as described (*S4, S6*).

Density plots. All DNA methylation kernel density plots compare fractional methylation within 50 bp windows. We used windows with at least 20 informative sequenced cytosines (10 for CHG in endosperm) and fractional methylation of at least 0.7 (CG), 0.4 (CHG endosperm), 0.5 (CHG pollen), 0.08 (CHH endosperm), 0.15 (CHH vegetative cell), or 0.05 (CHH sperm) in at least one of the samples being compared. For parent-of-origin endosperm plots, only windows with methylation differences between Col and L*er* below 0.1 (CG), 0.15 (CHG), or 0.05 (CHH) were used to exclude ecotype-specific differences. Windows in which fractional paternal (or sperm) CG methylation exceeded fractional maternal (or vegetative cell) CG methylation by at least 0.4 were considered demethylated.

Box plots. Box plots compare fractional methylation in TEs within 50 bp windows and use the same cutoffs as density plots. To examine the correlation between CG demethylation and chromatin structure, TE windows are separated into five groups in ascending order according to GC ratio, nucleosome enrichment, dimethylation of lysine 9 of histone H3 (H3K9me2), and distance from the closest edge of the TE, respectively. The five groups are as follows: for GC ratio, 0.2-0.3, 0.3-0.35, 0.35-0.4, 0.4-0.45, and >0.45; for nucleosome enrichment, 1-8, 9-16, 17-24, 25-39, and >39 counts (*S7*); for H3K9me2, <0.5, 0.5-1.25, 1.25-2, 2-3, and >3 $\log_2$ (IP/input) (*S8*); for distance to TE edge, <50 bp, 50-100 bp, 100-150 bp, 150-200 bp, and 200-250 bp.

Artificial microRNA transgene construction and analysis. We used the *AGL61* promoter to express an artificial microRNA directed against the *GFP* transcript specifically in the central cell (*S9*). The *AGL61* promoter was PCR amplified from Col-0 genomic DNA using the primers AGL61F-salI (5'-TGATTACGCCGTCGACAGATGATTTTAGAGTCTCCCGC-3') and AGL61R-asc1 (5'- CTCACCATGGCGCGCCTGTAACATACATTTGTAATTACTCG-3'). The *AGL61* promoter was then cloned into the *LAT52p-amiRNA=GFP* plasmid described in (*S10*), replacing the *LAT52* promoter at the SalI and AscI sites to create the *AGL61p-amiRNA=GFP* transgene. As a negative control, the *amiRNA-GFP* fragment was removed by EcoRI digestion followed by self-ligation of the remaining plasmid to create the *AGL61p* transgene. As a positive control, we used the *DD45* promoter to express an artificial microRNA directed against the *GFP* transcript specifically in the egg cell (*S11*). The *DD45* promoter was amplified from Col-0 genomic DNA using primers DD45F-SalI (5'-GACTGTCGACTAAATGTTCCTCGCTGACGT-3') and DD45R-AscI (5'-CTAGGCGCGCCTGTGTTAGAAGCCATTATTC-3'). The DD45 promoter was inserted into the *LAT52p-amiRNA=GFP* plasmid, replacing the *LAT52* promoter at the SalI and AscI sites to create the *DD45p-amiRNA=GFP* transgene.

Transgenic lines and microscopy analysis. Using Agrobacterium-mediated floral dip transformation (*S12*), the *AGL61p-amiRNA=GFP*, *AGL61p*, or *DD45p-amiRNA=GFP* transgenes were transformed into a *DD45p-GFP* homozygous reporter line that expresses GPF specifically in the egg cell (*S11*). Transgenic seeds were selected on plates with hygromycin antibiotic. PCR procedures were used to detect the presence of the *AGL61p-amiRNA=GFP*, *AGL61p*, or *DD45p-amiRNA=GFP* transgenes as well as the *DD45p-GFP* reporter transgene in hygromycin-resistant T1 seedlings. We monitored the intensity of GFP fluorescence in T1 plants.

Anthers were removed from stage 12 to 13 flower buds to prevent fertilization (*S13*). Carpels were dissected 48 hours later and GFP fluorescence in intact unfertilized ovules was observed as described previously (*S14*). GFP intensity was visually scored and grouped into two categories: strong GFP fluorescence versus faint or no GFP fluorescence.

References

S1. Y. Choi *et al.*, *Cell* **110**, 33 (2002).
S2. V. K. Schoft *et al.*, *Proc Natl Acad Sci U S A* **108**, 8042 (2011).
S3. V. K. Schoft *et al.*, *EMBO Rep* **10**, 1015 (2009).
S4. T.-F. Hsieh *et al.*, *Science* **324**, 1451 (2009).
S5. T. F. Hsieh *et al.*, *Proc Natl Acad Sci U S A* **108**, 1755 (2011).
S6. A. Zemach, I. E. McDaniel, P. Silva, D. Zilberman, *Science* **328**, 916 (2010).
S7. R. K. Chodavarapu *et al.*, *Nature* **466**, 388 (2010).
S8. Y. V. Bernatavichute, X. Zhang, S. Cokus, M. Pellegrini, S. E. Jacobsen, *PLoS One* **3**, e3156 (2008).
S9. J. G. Steffen, I. H. Kang, M. F. Portereiko, A. Lloyd, G. N. Drews, *Plant Physiol* **148**, 259 (2008).
S10. R. K. Slotkin *et al.*, *Cell* **136**, 461 (2009).
S11. J. G. Steffen, I.-H. Kang, M. Macfarlane, G. N. Drews, *Plant J* **51**, 281 (2007).
S12. K. S. Century *et al.*, *Science* **278**, 1963 (1997).
S13. D. R. Smyth, J. L. Bowman, E. M. Meyerowitz, *Plant Cell* **2**, 755 (1990).
S14. R. Yadegari *et al.*, *Plant Cell* **12**, 2367 (2000).

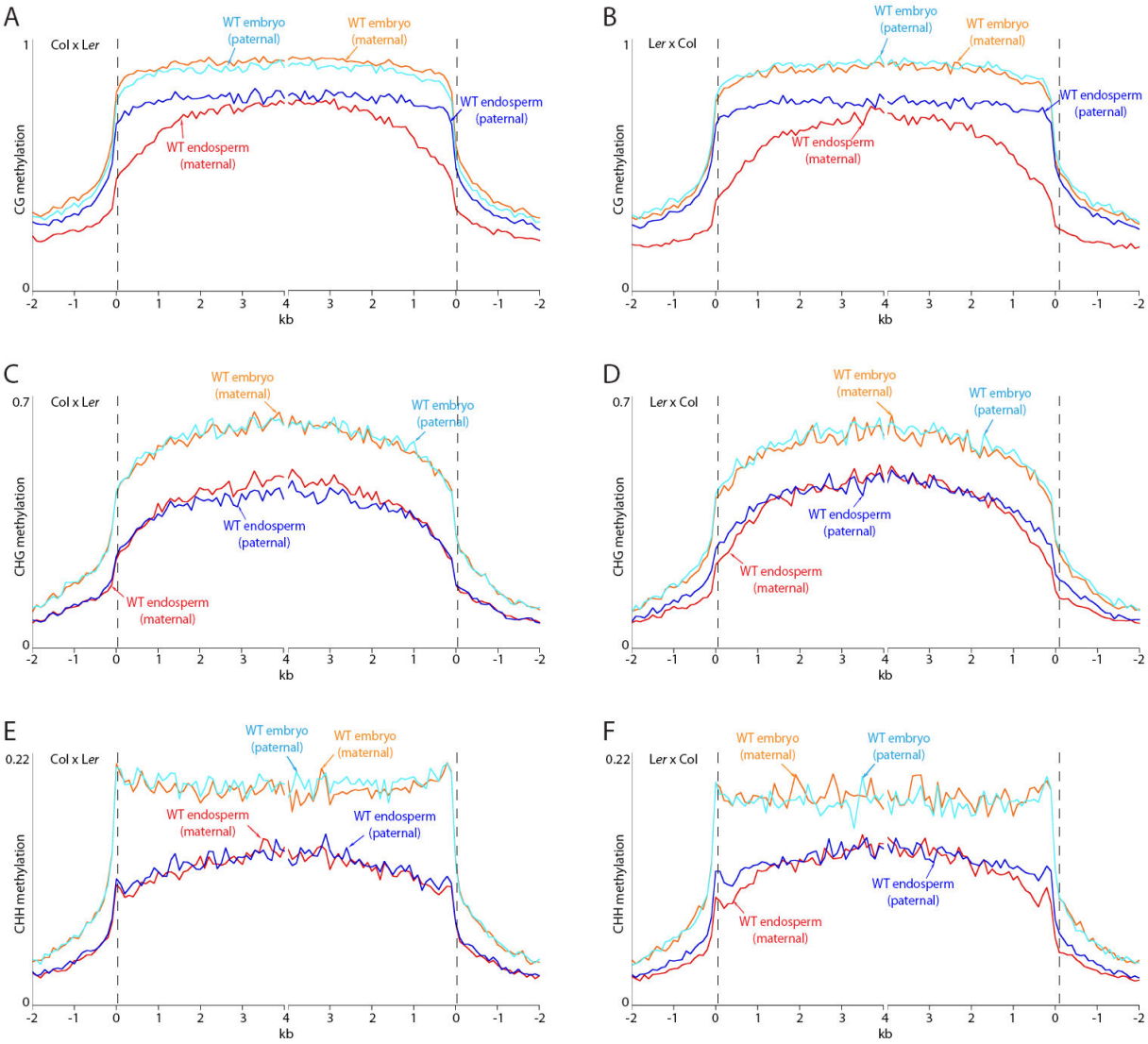

fig. S1. DNA methylation in *A. thaliana* transposons. (**A-F**) *A. thaliana* transposons were aligned at the 5' end (left panel) or the 3' end (right panel) and average methylation levels for each 100-bp interval are plotted for endosperm and embryo derived from Col x L*er* F1 seeds (**A, C, E**) and L*er* x Col F1 seeds (**B, D, F**). The dashed line at zero represents the point of alignment. CG methylation is shown in (**A-B**), CHG in (**C-D**), CHH in (**E-F**).

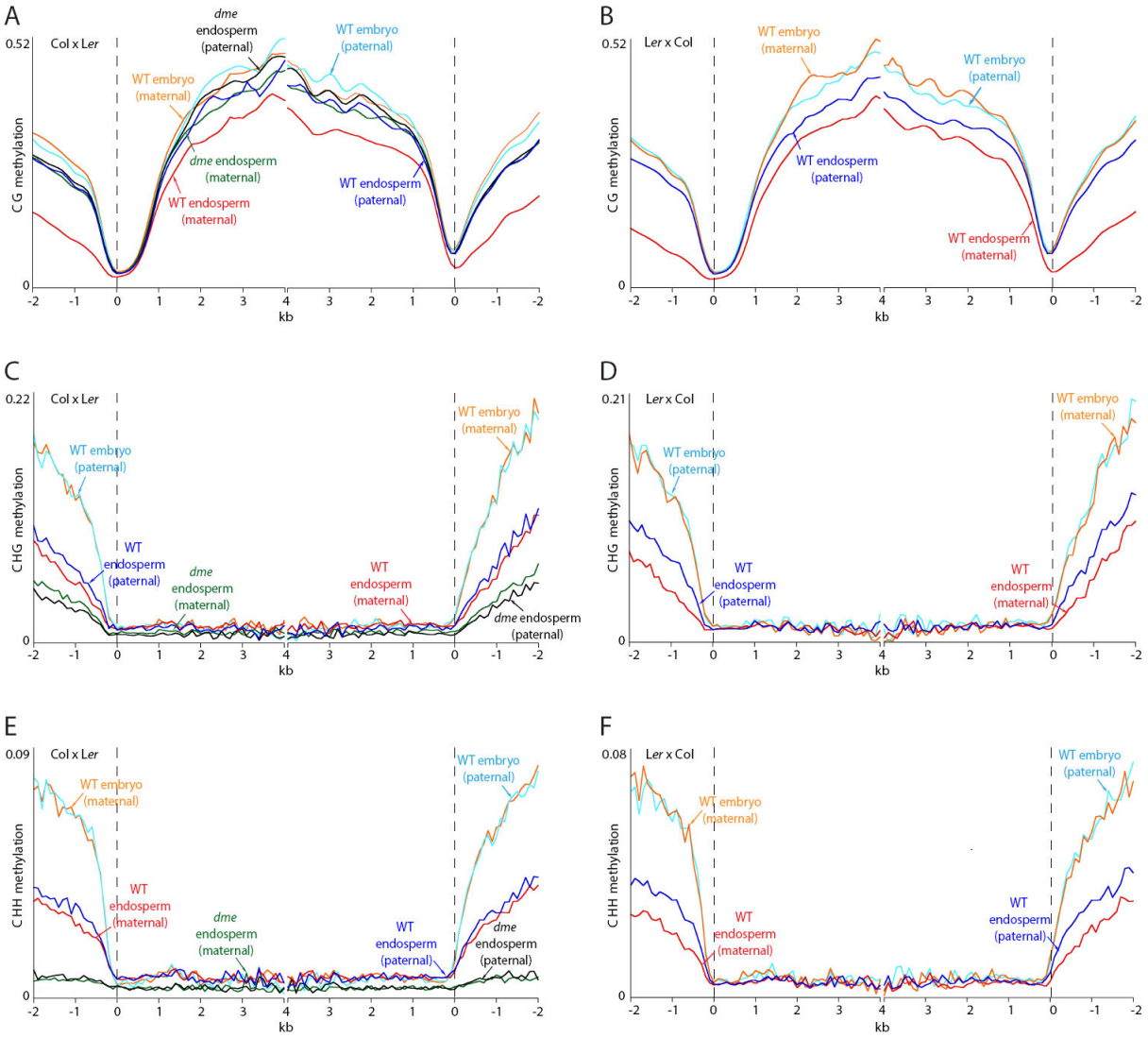

fig. S2. DNA methylation in *A. thaliana* genes. (**A-F**) *A. thaliana* genes were aligned at the 5' end (left panel) or the 3' end (right panel) and average methylation levels for each 100-bp interval are plotted for endosperm derived from Col x L*er* and *dme-2* (Col) x L*er* F1 seeds, and embryo derived from Col x L*er* seeds (**A, C, E**), and for endosperm and embryo derived from L*er* x Col F1 seeds (**B, D, F**). The dashed line at zero represents the point of alignment. CG methylation is shown in (**A-B**), CHG in (**C-D**), CHH in (**E-F**).

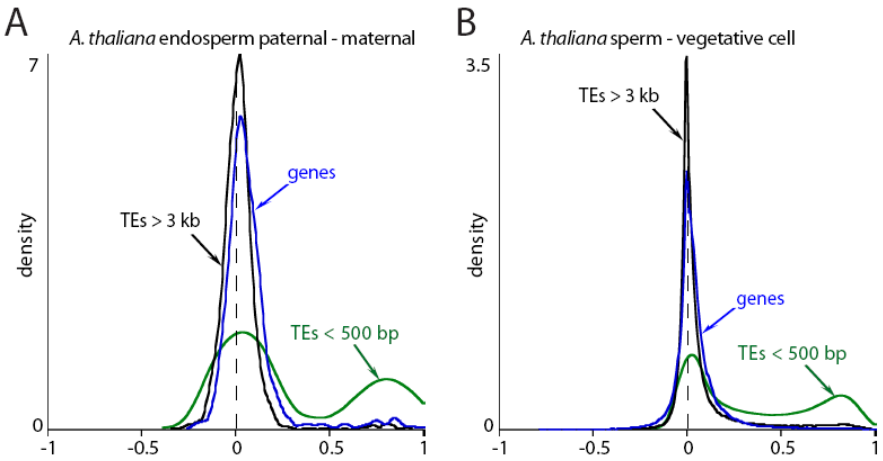

fig. S3. Maternal demethylation in genes and transposons (TEs). (**A-B**) Kernel density plots, which have the effect of tracing the frequency distribution, of the differences between *A. thaliana* paternal and maternal endosperm CG methylation (**A**), and sperm and vegetative cell CG methylation (**B**).

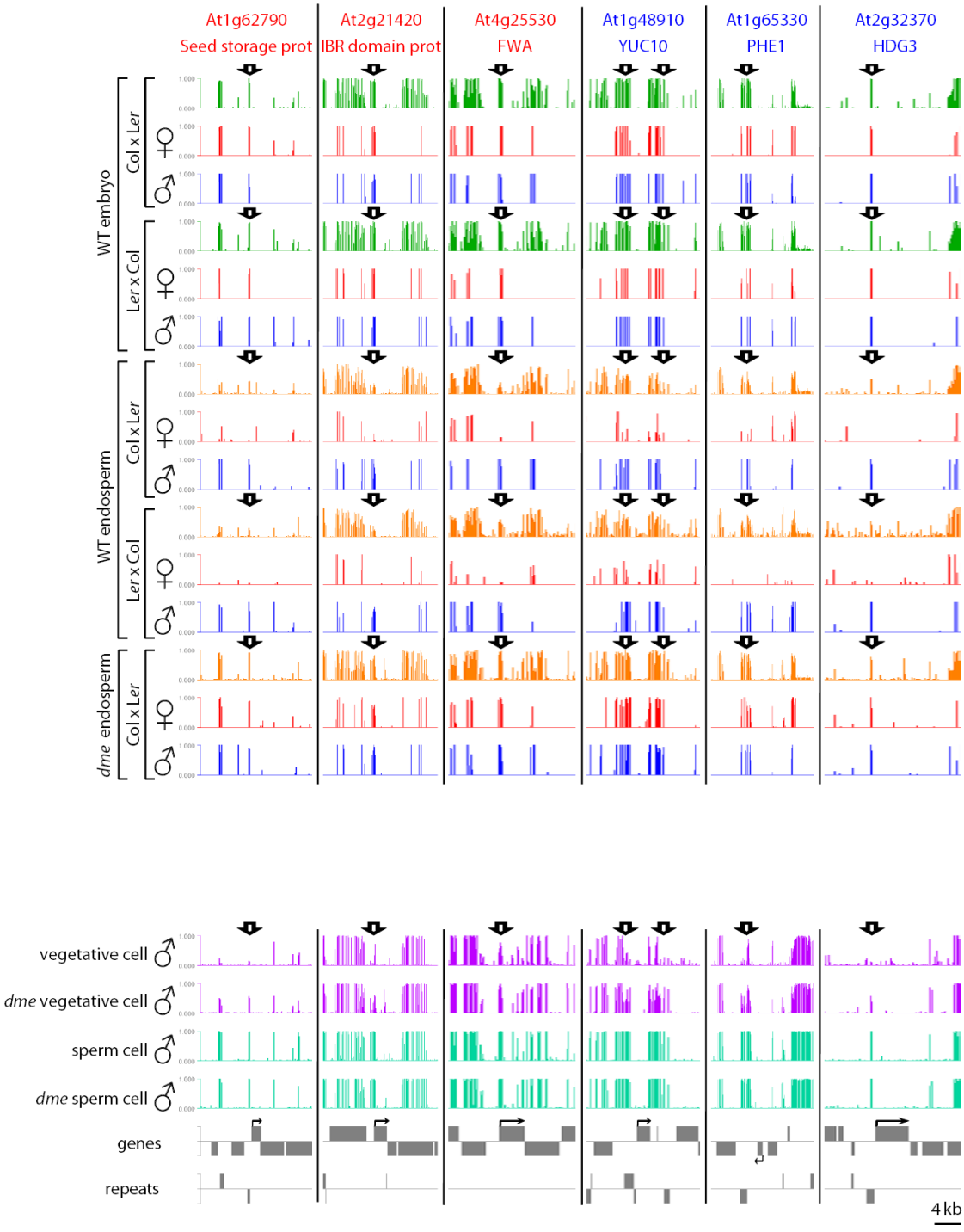

fig. S4. CG methylation near *A. thaliana* imprinted genes. Snapshots of CG methylation in indicated tissues near maternally expressed (red) and paternally expressed (blue) *A. thaliana* imprinted genes. Green bars represent embryo methylation, orange bars represent endosperm methylation, and red and blue bars represent methylation of the maternal and paternal genomes, respectively. Arrows point out methylation changes in endosperm and vegetative cell.

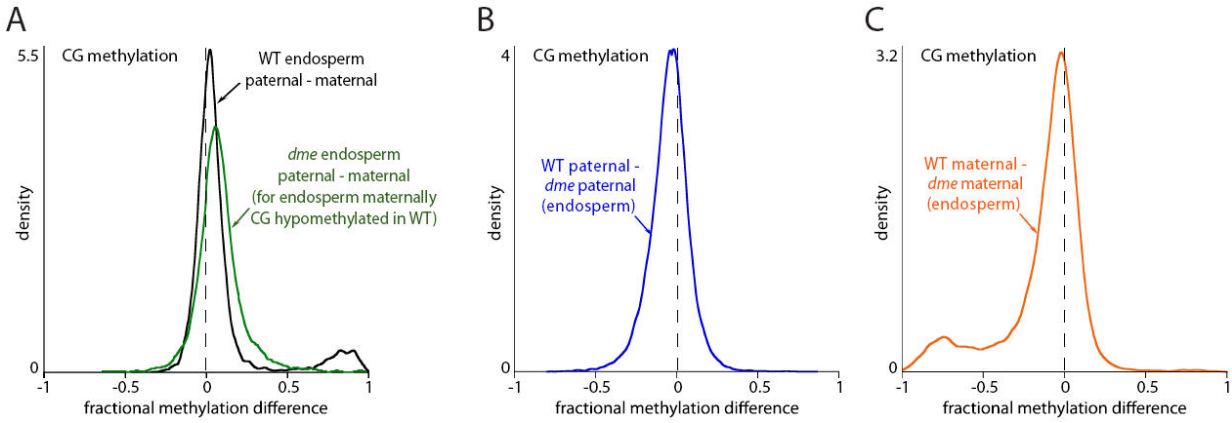

fig. S5. DNA methylation in *dme* endosperm. (**A-C**) Kernel density plots, which have the effect of tracing the frequency distribution, of the *A. thaliana* CG methylation differences between the indicated endosperm genomes.

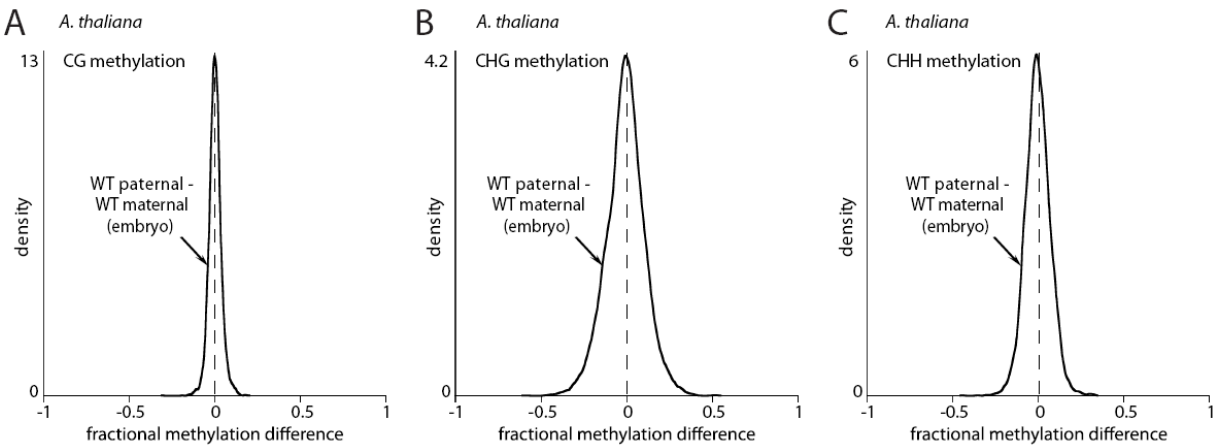

fig. S6. DNA methylation in *A. thaliana* embryo. (**A-C**) Kernel density plots, which have the effect of tracing the frequency distribution, of the differences between paternal and maternal embryo methylation in *A. thaliana*.

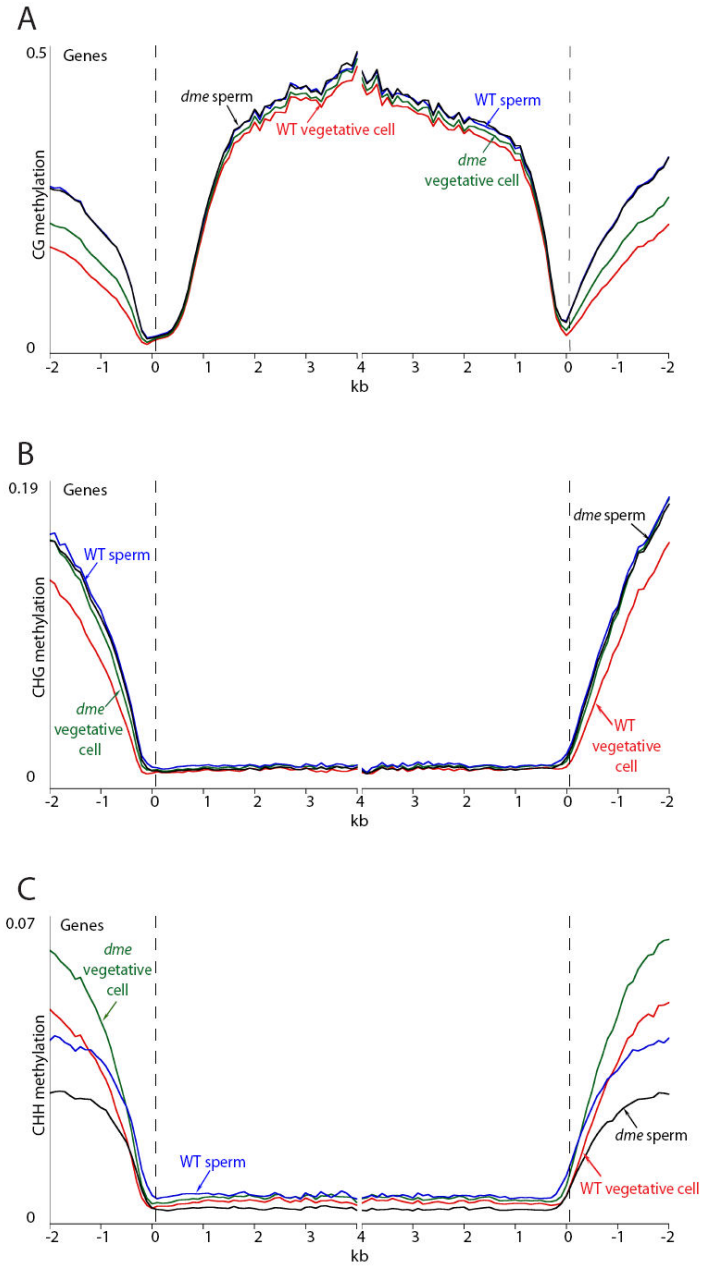

fig. S7. Pollen DNA methylation in genes for wild type and *dme-2*. (**A-C**) *A. thaliana* genes were aligned at the 5' end (left panel) or the 3' end (right panel) and average methylation levels for each 100-bp interval are plotted for vegetative and sperm cell genomes derived from wild-type and *dme-2*/+ pollen. The dashed line at zero represents the point of alignment. CG methylation is shown in (**A**), CHG in (**B**), CHH in (**C**).

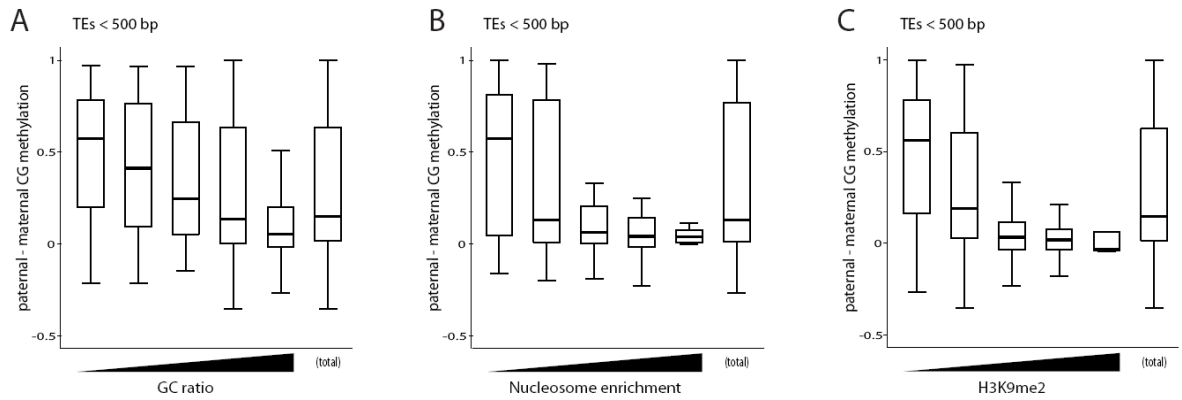

fig. S8. DNA demethylation in transposons. (**A-C**) Box plots showing fractional methylation differences between the paternal and maternal endosperm genomes in TEs within 50 bp windows. Each box encloses the middle 50% of the distribution, with the horizontal line marking the median. The lines extending from each box mark the minimum and maximum values that fall within 1.5 times the height of the box.

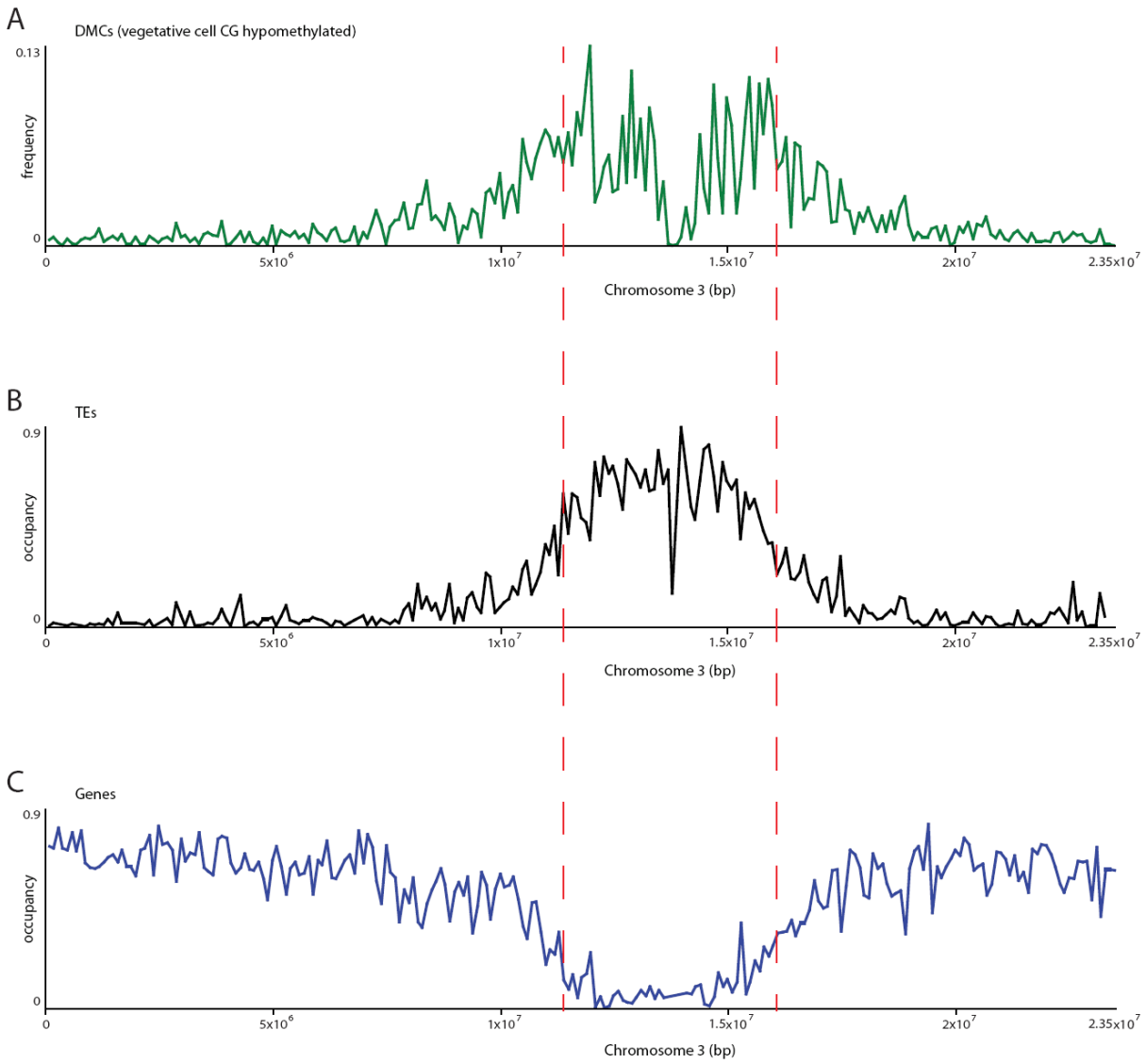

fig. S9. Distribution of CG sites demethylated in *A. thaliana* vegetative nuclei. (**A-C**) Distribution across *A. thaliana* chromosome 3 of significantly differentially methylated cytosines (DMCs; p-value < 0.0001, Fisher's exact test) in the CG context that are less methylated in wild-type vegetative cells than in sperm (**A**), transposable elements (**B**), and genes (**C**). The dashed lines roughly mark the boundaries of pericentric heterochromatin.

Sample	Median Coverage	Nuclear CG	Nuclear CHG	Nuclear CHH	Chloroplast CHH	M/P ratio
Col x L*er* embryo	5	29.2%	11.8%	4.6%	0.1%	0.96
L*er* x Col embryo	11	29.6%	12.1%	5.1%	0.1%	0.93
Col x L*er* endosperm	20	23.7%	8.7%	3.4%	0.4%	1.99
L*er* x Col endosperm	29	22.6%	8.6%	3.0%	0.1%	1.95
dme-2 x L*er* endosperm	22	27.2%	4.7%	0.7%	0.2%	2.09
WT vegetative cell	33	26.9%	13.0%	4.0%	0.3%	NA
WT sperm cell	37	31.2%	12.7%	2.1%	0.6%	NA
dme-2/+ vegetative cell	45	28.7%	14.1%	4.7%	0.3%	NA
dme-2/+ sperm cell	40	31.0%	12.4%	1.5%	0.3%	NA

Table S1. Median coverage per cytosine and mean DNA methylation for the indicated samples. Chloroplast CHH methylation is a measure of cytosine non-conversion and other errors. M/P = maternal/paternal; the expected ratio is 1 for embryo and 2 for endosperm. NA = not applicable.

Line	Transgene	No or faint GFP	Strong GFP	N	%	χ^2	P
1	*AGL61p-amiRNA=GFP*	118	102	220	53	1.16	> 0.28
2		106	96	202	52	0.50	> 0.48
3		100	91	181	55	1.00	> 0.31
4		104	112	216	48	0.15	> 0.79
5		105	107	212	49	0.01	> 0.92
6	*AGL61p*	14	199	213	6	-	-
7		16	202	218	7	-	-
8		7	210	217	3	-	-
9		14	201	215	6	-	-
10		15	207	222	6	-	-
11	*DD45p-amiRNA=GFP*	84	130	214	40	10	> 0.005
12		65	50	115	56	2	> 0.16
13		97	105	202	48	0.3	> 0.31

Table S2. The indicated transgenes were introduced into lines homozygous for the *DD45p-GFP* reporter gene that expresses *GFP* in the egg cell (*S11*). The *AGL61p-amiRNA=GFP* transgene specifically expresses in the central cell (*S9*) an artificial microRNA that targets *GFP* RNA. The *AGL61p* transgene is a negative control. The *DD45p-amiRNA=GFP* transgene is a positive control that specifically expresses in the egg cell (*S11*) the artificial microRNA that targets GFP RNA. After meiosis, a single hemizygous transgene in the primary T1 line is inherited by 50% of the female gametophytes. If the transgene silences the *DD45p-GFP* reporter, we would expect to detect 50% of the egg cells with strong GFP fluorescence and 50% of the egg cells with faint or no GFP fluorescence. We observed this result in the *AGL61p-amiRNA=GFP* and positive control *DD45p-amiRNA=GFP* transgenic lines, but not in the negative control *AGL61p* transgenic lines. N, number of egg cells examined. %, percentage of egg cells with no or faint GFP fluorescence. χ^2, calculated for a 1:1 segregation of egg cells with no or faint GFP fluorescence versus strong GFP fluorescence. P, probability that the deviation from the expected 1:1 segregation is due to chance.